Hindawi
International Journal of Aerospace Engineering
Volume 2020, Article ID 5247257, 11 pages
https://doi.org/10.1155/2020/5247257

Research Article

A Guidance Strategy for Strapdown Seeker considering Minimum Field-of-View Angle Constraint

Guanqun Zhou and Qunli Xia

School of Aerospace Engineering, Beijing Institute of Technology, Beijing 100081, China

Correspondence should be addressed to Guanqun Zhou; zhougq5307@163.com

Received 4 February 2020; Revised 26 May 2020; Accepted 28 May 2020; Published 19 June 2020

Academic Editor: Giulio Avanzini

An off-axis strapdown seeker in missile may lead to a minimum field-of-view (FOV) angle constraint problem. The goal of this paper is to deal with the problem in guidance. Analysis of kinematics proves that on the premise of attacking stationary target, seeker look angle comes to 0 before or at the end time, and seeker will lose target finally. In order to reduce the distance of seeker losing target, a guidance strategy is proposed to sustain minimum FOV angle constraint during flight. The strategy can be applied on guidance laws with independent orders in longitudinal and lateral channels. By means of a certain rolling maneuver, it keeps the target in the seeker's limited FOV. Moreover, a lateral guidance order compensation is utilized in the strategy to maintain seeker look angle. Simulations and comparisons are conducted to demonstrate the strategy's effectiveness. Results show that the guidance strategy can sustain minimum FOV angle constraint longer than classical guidance method.

1. Introduction

In recent years, strapdown seekers are widely used in hypersonic missiles. Usually, a seeker is installed in the nose of a missile, and the seeker axis is aligned with the missile body axis. In this scenario, the seeker's field-of-view (FOV) is symmetric around the body axis. However, there are some hypersonic aerodynamic configurations with a sharp nose. These configurations have narrow space in the nose, for which some large-sized seeker cannot be installed in a normal way. Only if the antenna is installed biased, the space is enough, as is shown in Figure 1.

An off-axis seeker's FOV is shown in Figure 1. The seeker axis is not aligned around the body axis, and all of the seeker's FOV lies in one side of the body. The body axis nearby is out of the seeker's FOV, which means once the missile points to a target in terminal guidance, the seeker cannot track the target. We can see from Figure 1 that in this special scenario, the seeker's FOV has both maximum angle and minimum angle constraints in missile's elevation direction.

So far to date, there is a lot of research on seeker maximum FOV angle constraint problem. In [1], a parameter design strategy for seeker FOV constraint in impact angle guidance is proposed. Based on optimal guidance law (OGL), it ensures that the look angle will not exceed the constraint boundary by changing guidance law parameters. This idea is well developed in [2], and an adaptive weighting impact angle optimal guidance law considering FOV angle constraint is presented in this paper. In addition to optimal guidance law, many modern guidance methods are applied to solve this problem. A nonsingular sliding-mode control guidance law considering FOV angle constraint is presented by [3]. By using slide mode control theory, this guidance law realizes impact time control as well as FOV angle control. An impact time control guidance law considering FOV angle constraint using backstepping control technique is proposed in [4]. This guidance law enables a reduced look angle in terminal guidance without violating the FOV angle limit. Moreover, a novel nonlinear mapping-based guidance strategy is presented in [5] for attacking stationary and moving targets, where the seeker's FOV constraint is transformed to the limit of the relative speed perpendicular to the LOS.

Those guidance laws mentioned are applied to solve the maximum FOV angle constraint problem, but they do not

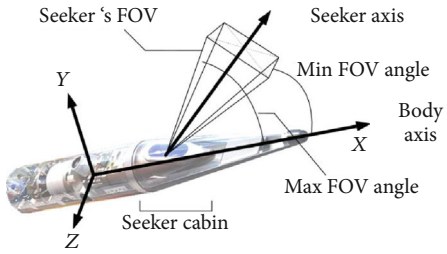

Figure 1: Hypersonic missile with an off-axis seeker.

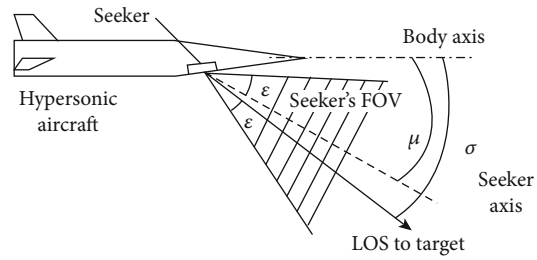

Figure 2: 2D angular configuration of the off-axis strapdown seeker.

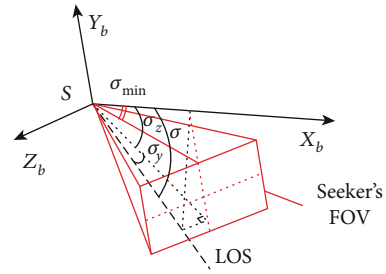

Figure 3: 3D angular configuration of the off-axis strapdown seeker.

control the minimum value of look angle in flight. Actually, on condition of hitting a stationary target, velocity heading error finally converges to 0 by using those guidance laws. This fact means those guidance laws cannot solve the minimum FOV angle constraint problem. Until now, there are few researches against minimum FOV angle constraint. Moreover, according to the following analysis in this paper, there is conflict between keeping a nonzero heading error at the terminal of trajectory and hitting a stationary target, which means that the minimum FOV angle constraint problem cannot be solved thoroughly. The seeker will finally lose the target in some distance.

However, even though it is impossible to solve the problem thoroughly, to reduce the distance of the seeker losing the target is still very meaningful to promote terminal guidance accuracy. From the point of this, a guidance strategy is designed and proposed by this paper to sustain seeker minimum FOV angle constraint. By means of this strategy, the distance of seeker losing the target decreases a lot. The rest of this paper is organized as follows. Section 2 introduces the problem of minimum FOV angle constraints and analyzes the restriction of minimum FOV angle control in terminal guidance. In Section 3, a guidance strategy based on traditional terminal guidance law is derived to maintain minimum FOV angle constraints in flight. Simulation results are presented in Section 4, and Section 5 gives conclusions.

2. Problem Formulation

2.1. Minimum FOV Angle Constraint Problem. Figure 2 describes a 2D angular configuration of an off-axis strapdown seeker. σ denotes the look angle, and μ denotes the seeker head angle. The range of the seeker's FOV is defined as $\pm\varepsilon$ (symmetric with seeker axis). Therefore, the range of effective seeker look angle is expressed as

$$\mu - \varepsilon \le \sigma \le \mu + \varepsilon. \tag{1}$$

For normal strapdown seeker whose axis is aligned with body axis, μ equals to zero. Seeker's FOV is symmetric with the body axis. Different from that, a biased strapdown seeker has a nonzero μ. On condition of $\mu > \varepsilon$, the value of $(\mu - \varepsilon)$ will be positive and the seeker's FOV is completely at one side of the body axis, as shown in Figure 2.

In convenience of expression, we define $\sigma_{\min} = \mu - \varepsilon$ and $\sigma_{\max} = \mu + \varepsilon$. Equation (1) can be written as

$$\sigma_{\min} \le \sigma \le \sigma_{\max}. \tag{2}$$

Equation (2) shows the complete constraint caused by a biased seeker's FOV in a 2D scenario. The left side of this equation shows a new constraint problem of minimum FOV angle. This constraint requires a nonzero look angle during guidance in order to sustain target in the seeker's FOV. It is totally different with the traditional maximum seeker's FOV angle constraint problem because the latter one only requires the absolute value of the seeker look angle within a certain range.

In a 3D scenario, this problem is more complex. Before we discuss it, two assumptions are adopted: (1) the seeker's FOV is assumed as a rectangular pyramid; (2) the seeker's FOV is symmetric with a longitudinal plane. Figure 3 presents the 3D scenario of an off-axis strapdown seeker. (X_b, Y_b, Z_b) represents the missile body frame, and S denotes the seeker. X_bSY_b plane represents the body longitudinal plane. In this figure, the seeker's FOV is represented as the red zone.

Basically, the definition of look angle σ in 3D is the space angle between LOS and seeker axis, and σ has no sign. In convenience of analysis, we can replace the space look angle by two Euler angles from LOS coordinate frame to body frame; then, the 3D look angle constraint problem can be transformed into two planar problems. In Figure 3, σ_y and σ_z represent the Euler angles in azimuth and elevation directions. According to their definition, both σ_y and σ_z have a sign.

Obviously, the seeker's FOV in azimuth and elevation directions is different. The former is symmetric with longitudinal axis, while the latter one is biased to one side. This paper focuses on look angle constraint problem in elevation channel. Under the assumption that azimuth and elevation guidance are independent, this problem is quite the same

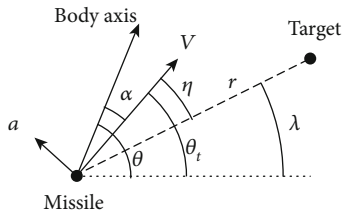

Figure 4: Engagement geometry of missile and a stationary target.

with the 2D scenario mentioned. The rest of this article will concentrate on dealing with this constraint problem in terminal guidance design. However, there exists some restriction in practice which makes it hard to sustain the look angle at a nonzero value all the time during terminal guidance. This point will be proposed in the following analysis.

2.2. Look Angle Control Restriction in Terminal Guidance. The commonly used engagement geometry of missile and a stationary target in the 2D scenario is shown in Figure 4, where V and r represent missile's velocity and relative distance to target. θ_t and λ represent trajectory inclination angle, velocity heading angle, and LOS angle. Missile's pitching angle and attack angle are defined as θ and α.

Dynamic equations are obtained as follows [6, 7].

$$\begin{cases} \dot{\theta}_t = \dfrac{a}{V}, \\ \dot{\lambda} = -\dfrac{\sin\eta}{r}, \\ \dot{\eta} = \dot{\theta}_t - \dot{\lambda} = \dfrac{a}{V} + \dfrac{\sin\eta}{r}, \end{cases} \tag{3}$$

where a represents normal acceleration regarded as control force of missile. The complete description of the look angle σ is obtained from Figure 4 as

$$\sigma = \theta - \lambda = \theta_t + \alpha - \lambda = \eta + \alpha. \tag{4}$$

Differentiating equation (4) and substituting equation (3) into it yields

$$\dot{\sigma} = \dot{\eta} + \dot{\alpha} = \frac{a}{V} + \frac{V\sin\eta}{r} + \dot{\alpha}. \tag{5}$$

From equation (5), we can see that velocity heading angle η converges to 0 when the missile hits the target at the end of trajectory. Otherwise, $\dot{\sigma}$ will be infinite and the look angle is divergent.

Defining terminal time as t_f, and $\eta(t_f) = 0$. Because η is continuous, there exists $\varepsilon > 0$, when $t \in [t_f - \varepsilon,\ t_f)$, η varies monotonically. Without loss of generality, we can assume that $\eta(t) > 0$ and $\dot{\eta}(t) \le 0$ when $t \in [t_f - \varepsilon,\ t_f)$. To ensure the establishment of equation (3), there must be $a(t) < 0$. Generally, we have sign (a) = sign (α); therefore, attack angle $\alpha(t) < 0$. There exists $t_1 \in (t_f - \varepsilon,\ t_f]$ when $\sigma(t_1) = \eta(t_1) + \alpha(t_1) = 0$. If $t_1 < t_f$, $\sigma(t)$ comes to 0 and keeps nonpositive during $t \in [t_1,\ t_f]$. If $t_1 = t_f$, $\sigma(t)$ converges to 0 along with $\eta(t)$. But in any case, $\sigma(t_f) \le 0$.

According to the above-mentioned analysis, the following conclusion is given:

(i) On the premise of hitting stationary target with a continuous normal acceleration, the value of the look angle σ will come to 0 before or at the end time

(ii) It is impossible to maintain the minimum FOV angle constraint all the time within a finite acceleration during terminal guidance

However, we can still determine a minimum distance r_e. When relative distance r is larger than r_e, the minimum FOV angle constraint can be maintained within a limited normal acceleration, and r_e is named as seeker look angle control end point.

In order to determine the end point r_e, the following Lyapunov function is constructed [8].

$$L = \frac{1}{2}\sigma^2. \tag{6}$$

Differentiating equation (6) with respect to time yields

$$\dot{L} = \sigma\dot{\sigma} = \sigma\left(\frac{a}{V} + \frac{V\sin\eta}{r} + \dot{\alpha}\right). \tag{7}$$

To ensure the stability of system (6), equation (7) should keep negative. If minimum FOV angle constraint boundary $\sigma_{\min}$ is positive, the condition of $\dot{L}$ is written as

$$\frac{a}{V} + \frac{V\sin\eta}{r} + \dot{\alpha} < 0. \tag{8}$$

When the missile flies in low altitude with a high speed, the dynamic pressure is very large, and a small attack angle can provide huge normal acceleration. In terminal guidance, we hope acceleration changes smoothly at the end, considering autopilot lag. Therefore, it is reasonable to assume a small rangeability of attack angle at the end of trajectory. Ignoring $\dot{\alpha}$ in equation (8), the following equation is obtained:

$$a < -\frac{V^2\sin\eta}{r} < 0. \tag{9}$$

We can assume that at the end of trajectory velocity is relatively constant, and the normal acceleration is constrained within the maximum value $a_{\max}$. Because in terminal guidance flight look angle is required larger than $\sigma_{\min}$, we obtain $\eta > \sigma_{\min}$ on this condition.

In order to maintain the establishment of equation (9), we have

$$r > \frac{V^2}{a_{\max}}\sin\sigma_{\min}. \tag{10}$$

Defining $r_e = (V^2 \sin \sigma_{\min})/a_{\max}$, we can set r_e as an end point of seeker look angle control. The meaning of this end point is shown as follows. When $r > r_e$, the minimum FOV angle constraint can be maintained with an acceleration command lower than $a_{\max}$. After that point, look angle control should be abandoned because the acceleration command might exceed limitation.

2.3. 3D Kinematic Model. Figure 5 shows a three-dimensional homing engagement geometry of missile to stationary target, where (X, Y, Z) denotes inertial coordinate system. M and T represent missile and target. r denotes relative distance between missile and target. V denotes total velocity of missile. Notations of λ_y and λ_z stand for LOS angles in azimuth and elevation directions. Notations of η_y and η_z represent Euler angles from the LOS coordinate system to the missile's velocity coordinate system.

The three-dimensional kinematics is given by the following equations [9–12].

$$\begin{aligned}
\dot{r} &= -V \cos \eta_z \cos \eta_y, \\
\dot{\lambda}_y &= -V \frac{\sin \eta_z}{r}, \\
\dot{\lambda}_z &= -V \frac{\sin \eta_z \cos \eta_y}{r \cos \lambda_z}, \\
\dot{\eta}_z &= \frac{a_z}{V} + \frac{V}{r}\left(\sin \eta_z \sin^2 \eta_y \tan \lambda_z + \sin \eta_z \cos \eta_y\right), \\
\dot{\eta}_y &= \frac{a_y}{V \cos \eta_z} - \frac{V}{r}\left(\sin \eta_z \sin \eta_y \cos \eta_z \tan \lambda_z - \frac{\sin \eta_y}{\cos \eta_z}\right),
\end{aligned} \tag{11}$$

where a_y and a_z stand for missile's azimuth and elevation acceleration in velocity coordinate. Two Euler angles η_y and η_z express the heading error of velocity. In convenience of analysis, many articles assume that missile's attack angle and sideslip angle are ignored. Therefore, η_y and η_z are the same as the seeker look angle. This assumption is reasonable when discussing the maximum FOV angle constraint. However, when we deal with the minimum FOV angle constraint problem, this assumption is not appropriate because values of attack angle or sideslip angle in terminal guidance might be close to the look angle's value on this condition. A strict expression of seeker look angle should be obtained. It is given in the next section.

3. Guidance Strategy Design considering Minimum FOV Angle Constraint

On the basis of conclusions obtained in the last section, for missiles whose seeker has constraint of minimum FOV angle, it is inevitable that the seeker will lose the target finally. The realistic solution of this problem is locating the target when it is within the seeker's FOV and calculating guidance information according to target coordinate. The accuracy of target location is affected by relative distance between missile and target. Reducing the distance of seeker losing target improves target location accuracy effectively and contributes to precision terminal guidance. In this section, a guidance strategy is proposed to satisfy minimum FOV angle constraint in flight. It is not aimed at designing a new form of guidance law. Instead, this strategy can be applied in most terminal guidance law.

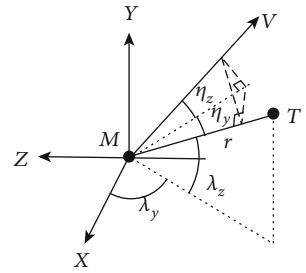

Figure 5: Three-dimensional homing engagement geometry.

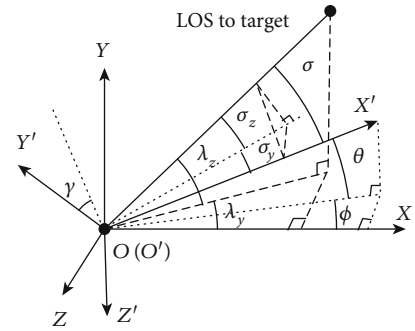

Figure 6: Angular relationships of missile and target in 3D.

3.1. Look Angle Characteristic Analysis. Figure 6 shows the three-dimensional homing engagement geometry of missile to target, where $O - XYZ$ denotes the inertial coordinate system and $O' - X'Y'Z'$ denotes the body coordinate system of missile. The inertial coordinate system is fixed on earth, and axis OY is vertical to the horizontal plane. The position of coordinate origin O can be defined as any appropriate value, as well as directions of axis OX and OZ in the horizontal plane. The coordinate origin O' of the body system is defined as missile's mass point. Axis $O'X'$ is defined as missile's body axis. Axis $O'Y'$ is defined in missile's longitudinal plane pointing upwards. Both inertial system and body system are right-handed coordinate system.

Notations of θ, ϕ, and γ stand for 3 Euler angles of pitching, yawing, and rolling angle from inertial system to body system. λ_z and λ_y represent LOS angles in elevation and azimuth directions. Moreover, σ_z and σ_y represent missile's look angles in elevation and azimuth directions of body system.

Coordinate transformation matrix from the inertial system to the body system $\mathbf{T}$ is shown as

$$\mathbf{T} = \mathbf{T}_x(\gamma)\mathbf{T}_y(\gamma)\mathbf{T}_z(\theta), \tag{12}$$

where $\mathbf{T}_x$, $\mathbf{T}_y$, and $\mathbf{T}_z$ are defined as

$$\mathbf{T}_x(*) = \begin{bmatrix} 1 & 0 & 0 \\ 0 & \cos * & \sin * \\ 0 & -\sin * & \cos * \end{bmatrix},$$
$$\mathbf{T}_y(*) = \begin{bmatrix} \cos * & 0 & -\sin * \\ 0 & 1 & 0 \\ \sin * & 0 & \cos * \end{bmatrix}, \quad (13)$$
$$\mathbf{T}_z(*) = \begin{bmatrix} \cos * & 0 & -\sin * \\ 0 & 1 & 0 \\ \sin * & 0 & \cos * \end{bmatrix}.$$

Assuming the unit vector of LOS represented in the body system and the inertial system are $\mathbf{e}_B$ and $\mathbf{e}_I$, it is easy to calculate that

$$\begin{cases} \mathbf{e}_B = \left[\mathbf{T}_z(\sigma_z)\mathbf{T}_y(\sigma_y)\right]^{-1}\mathbf{e}, \\ \mathbf{e}_I = \left[\mathbf{T}_z(\lambda_z)\mathbf{T}_y(\lambda_y)\right]^{-1}\mathbf{e}, \end{cases} \quad (14)$$

where $\mathbf{e}$ represents the unit vector of $[1\,0\,0]^T$. According to the coordinate transformation between the inertial system and the body system, we have

$$\mathbf{e}_B = \mathbf{T}\mathbf{e}_I. \quad (15)$$

By substituting equation (15) into (12), the following equation is obtained

$$\begin{cases} \cos\sigma_y \cos\sigma_z = \sin\theta \cos\left(\phi - \lambda_y\right)\cos\lambda_z + \cos\theta \sin\lambda_z, \\ \sin\sigma_z = A\cos\gamma + B\sin\gamma, \\ \sin\sigma_y \cos\sigma_z = -A\sin\gamma - B\cos\gamma, \end{cases} \quad (16)$$

where A and B are defined as

$$\begin{cases} A = -\sin\theta\cos\left(\phi - \lambda_y\right)\cos\lambda_z + \cos\theta\sin\lambda_z, \\ B = \sin\left(\phi - \lambda_y\right)\cos\lambda_z. \end{cases} \quad (17)$$

The angle σ is defined as heading error between LOS and body axis. According to Figure 6, it can be obtained as

$$\sigma = \cos^{-1}\left(\cos\sigma_z \cos\sigma_y\right). \quad (18)$$

It is easy to know that $|\sigma_z|$ is no more than σ. Substituting the first equation of equation (16) into equation (18) yields

$$|\sigma_z| \le \sigma = \cos^{-1}\left[\sin\theta\cos\left(\phi - \lambda_y\right)\cos\lambda_z + \cos\theta\sin\lambda_z\right]. \quad (19)$$

Noticing that $A^2 + B^2 + \cos^2\sigma = 1$, we can get $A^2 + B^2 = \sin^2\sigma$. Substituting equation (19) into the second line of equation (16), the following equation is obtained:

$$\sin\sigma_z = \sin\sigma\left[\frac{A}{\sqrt{A^2+B^2}}\cos\gamma + \frac{B}{\sqrt{A^2+B^2}}\sin\gamma\right]. \quad (20)$$

Furthermore, we can define γ^* as

$$\gamma^* = \begin{cases} \tan^{-1}(B/A), & A > 0, \\ \pi + \tan^{-1}(B/A), & A \le 0, \end{cases} \quad (21)$$

and equation (20) is simplified as

$$\sin\sigma_z = \sin\sigma\cos\left(\gamma - \gamma^*\right). \quad (22)$$

According to equation (22), the following conclusion is obtained. Under a certain condition of body axis and LOS orientations, the range of σ_z is restricted to $[-\sigma, \sigma]$, and only when rolling angles γ equals γ^* the maximum value is obtained. σ and γ^* can be calculated by equations (18) and (21).

On condition that the required minimum look angle $\sigma_{\min}$ ($\sigma_{\min} > 0$) is less than σ, it is derived from equation (22) that in order to keep $\sigma_z \ge \sigma_{\min}$, rolling angles γ should satisfy

$$\cos\left(\gamma - \gamma^*\right) \ge \frac{\sin|\sigma_{\min}|}{\sin\sigma}. \quad (23)$$

Defining

$$\Delta\gamma = \cos^{-1}\left(\frac{\sin|\sigma_{\min}|}{\sin\sigma}\right), \quad (24)$$

equation (23) is rewritten as

$$\gamma^* - \Delta\gamma \le \gamma \le \gamma^* + \Delta\gamma. \quad (25)$$

Equation (25) indicates that the range of γ satisfying the constraint of $\sigma_{\min} < \sigma_z$ is symmetric to γ^*. If $\sigma_{\min}/\sigma_z \to 1$, the value of $\Delta\gamma$ converges to 0.

The aforementioned analysis is based on a positive $\sigma_{\min}$. In practice, sometimes $\sigma_{\min}$ is defined negative. On this condition, the minimum FOV angle constraint is expressed as $\sigma_z < \sigma_{\min} < 0$, and equation (25) is rewritten as

$$\pi + \gamma^* - \Delta\gamma \le \gamma \le \pi + \gamma^* + \Delta\gamma. \quad (26)$$

3.2. Design of Guidance Strategy. The main scheme of this strategy is depicted as follows:

(i) If the current value of $|\sigma_z|$ is no less than $|\sigma_{\min}|$, it follows the order of the existing guidance law in flight

(ii) If the current value of $|\sigma_z|$ is less than $|\sigma_{\min}|$, while LOS heading error $\sigma \ge |\sigma_{\min}|$, the strategy will generate a rolling maneuver order to sustain the

minimum FOV angle constraint. On this condition, acceleration orders given by guidance law are kept, but they should be rewritten in body frame

(iii) If LOS heading error $\sigma \geq |\sigma_{\min}|$, the strategy gives a new guidance order in the azimuth direction as a lateral maneuver, and guidance order in the elevation direction is maintained

The following analysis will introduce the strategy in detail.

3.2.1. Basic Guidance Law. In the problem formulation part, we transform the 3D look angle constraint problem into two planar problems. This simplification requires a hidden assumption. Terminal guidance can be separated into two independent parts, longitudinal guidance and lateral guidance. Therefore, the guidance strategy proposed by this paper can be applied in the situation that guidance orders of longitudinal channel and lateral channel are given independently, like most classical guidance law.

In general, terminal guidance of air-to-surface missile has a constraint of impact angle in elevation direction to improve impact effect. Without a loss of generality, we can assume that in terminal guidance missile adopts optimal guidance law (OGL) [12, 13] with impact angle constraint in elevation direction, while azimuth guidance adopts proportional navigation guidance (PNG) [14] law to ensure hitting the target. Guidance order of acceleration in elevation a_{yc} and azimuth order a_{zc} is obtained as follows.

$$\begin{cases} a_{yc} = N_p V \dot{\lambda}_z + N_q V \left(\lambda_z - \theta_f\right)/t_{\text{go}}, \\ a_{zc} = -NV\dot{\lambda}_y, \end{cases} \tag{27}$$

where N_p and N_q are designer-chosen gain of OGL and N is designer-chosen gain of PNG law. Values of N_p, N_q, and N are chosen as 4, 2, and 4 in this paper [15]. t_{go} and θ_f represent time-to-go and predetermined impact angle.

It is noticed that a_{yc} and a_{zc} are given in the LOS frame [16–18]. An order transformation to body frame is necessary for autopilot in missile. Equation (28) gives a simplified transformation. This simplification is acceptable in practice when the magnitude of heading error σ is not very large.

$$\begin{cases} a_{ybc} = a_{yc} \cos\gamma + a_{zc} \sin\gamma, \\ a_{zbc} = a_{zc} \cos\gamma - a_{yc} \sin\gamma. \end{cases} \tag{28}$$

In equation (28), γ represents current rolling angle. a_{ybc} and a_{zbc} are acceleration order defined in pitching and yawing channel of body coordinate frame. In fact, a_{ybc} and a_{zbc} are direct inputs of autopilot, as well as rolling angle order γ_c.

3.2.2. Look Angle Compensation Strategy. According to equation (18), if the required minimum look angle $\sigma_{\min}$ is no larger than σ, the constraint of $\sigma_z \geq \sigma_{\min}$ can be sustained as long as the rolling angle is within range described by equation (25) or (26).

On the other hand, if σ is less than $\sigma_{\min}$, σ_z will never satisfy the constraint no matter how the rolling angle changes. On this condition, the most important work is to enlarge σ. It is obtained from equation (19) that

$$\cos\left(\phi - \lambda_y\right) = \frac{\cos\sigma - \sin\theta \sin\lambda_z}{\cos\theta \cos\lambda_z}. \tag{29}$$

The left side of equation (29) is only related to yawing angle ϕ and LOS azimuth angle λ_y, while the right side is influenced by pitching angle θ, LOS azimuth angle λ_z, and σ. Under normal condition, σ, θ, and λ_z are all within $[-90^\circ, 90^\circ]$; substituting $\sigma_{\min} < \sigma_z$ into equation (29) yields

$$\cos\left(\phi - \lambda_y\right) < \frac{\cos\sigma_{\min} - \sin\theta \sin\lambda_z}{\cos\theta \cos\lambda_z}. \tag{30}$$

The inequality given by equation (30) shows the constraint of minimum FOV angle on missile's attitude angle. If we want to enlarge σ, one effective way is to enlarge the difference between ϕ and λ_y. The inequality of equation (30) can also be converted into the following form.

$$\left|\phi - \lambda_y\right| > \cos^{-1}\left(\frac{\cos\sigma_{\min} - \sin\theta \sin\lambda_z}{\cos\theta \cos\lambda_z}\right). \tag{31}$$

In convenience of expression, we can define $\Delta\phi$ as

$$\Delta\phi = \cos^{-1}\left(\frac{\cos\sigma_{\min} - \sin\theta \sin\lambda_z}{\cos\theta \cos\lambda_z}\right), \tag{32}$$

and equation (31) is simplified as

$$\left|\phi - \lambda_y\right| > \Delta\phi. \tag{33}$$

The above analysis shows that if we want to keep $\sigma > \sigma_{\min}$, we can sustain yawing angle ϕ in the range shown by equation (33) without changing pitching angle θ. This approach only changes azimuth guidance order to compensate the look angle in necessity. It will not influence elevation guidance.

From the above, a guidance strategy that compensates the look angle is obtained. The main flow of this strategy is described as follows:

Step 1. Former guidance law gives orders both in elevation and azimuth directions as a_{yc} and a_{zc}. The rolling angle order is also given as γ_c.

Step 2. Calculating heading error angle between LOS and body axis as σ by equation (19). If $\sigma > |\sigma_{\min}|$, the flow goes to branch of Step 3; otherwise, it goes to Step 4.

Step 3. Calculating γ^* and $\Delta\gamma$ by equations (21) and (24). Updating rolling angle order by the following equation:

$$\sigma_{\min} \geq 0, \quad \gamma_c' = \begin{cases} \gamma_c, & |\gamma_c - \gamma^*| < \Delta\gamma, \\ \gamma^* - \Delta\gamma, & (\gamma_c - \gamma^*) < -\Delta\gamma, \\ \gamma^* + \Delta\gamma, & (\gamma_c - \gamma^*) > \Delta\gamma, \end{cases} \tag{34}$$

$$\sigma_{\min} < 0, \quad \gamma_c' = \begin{cases} \gamma_c, & |\gamma_c - \pi - \gamma^*| < \Delta\gamma, \\ \gamma^* + \pi - \Delta\gamma, & (\gamma_c - \pi - \gamma^*) < -\Delta\gamma, \\ \gamma^* + \pi + \Delta\gamma, & (\gamma_c - \pi - \gamma^*) > \Delta\gamma, \end{cases} \tag{35}$$

where γ_c' is the updated rolling angle order by the strategy.

Updating acceleration orders both in elevation and azimuth directions by the following equation:

$$\begin{cases} a_{yc}' = a_{yc}, \\ a_{zc}' = a_{zc}, \end{cases} \tag{36}$$

where a_{yc}' and a_{zc}' are updated acceleration orders by the strategy. Thus, a_{yc}', a_{zc}', and γ_c' constitute outputs of the guidance system.

Step 4. Calculating γ^* by equation (21). Updating the rolling angle order by the following equation:

$$\gamma_c' = \gamma^*, \tag{37}$$

where γ_c' is the updated rolling angle order by the strategy.

Calculating the expected yawing angle by the following equation:

$$\phi_c = \begin{cases} \lambda_y + \Delta\phi, & \phi \geq \lambda_{y,} \\ \lambda_y - \Delta\phi, & \phi < \lambda_y, \end{cases} \tag{38}$$

where $\Delta\phi$ is obtained from equation (32).

Generating new acceleration orders by the following equation:

$$\begin{cases} a_{yc}' = a_{yc}, \\ a_{zc}' = a_{zc} + K(\phi_c - \phi), \end{cases} \tag{39}$$

where K is a guidance coefficient. To determine the value of K, one needs to know the dynamics of original lateral guidance loop. If the guidance loop is approximate to a first-order system and time constant is T, coefficient K in equation (39) should be larger than V/T so that the additional guidance order $K(\phi_c - \phi)$ will not influence the original guidance loop.

It is indicated from equation (39) that azimuth guidance order is compensated to adjust the yawing angle so that a larger look angle σ is sustained. Thus, a_{yc}', a_{zc}', and γ_c' constitute the output of guidance system.

Table 1: Algorithm of the guidance strategy.

Step 1	Guidance order obtained as a_{yc}, a_{zc}, and γ_c
Step 2	Calculating heading error angle σ from equation (19)
If $\sigma \geq \lvert\sigma_{\min}\rvert$	
Step 3	Calculating γ^* and $\Delta\gamma$ by equation (21) and equation (24)
	Updating rolling angle order as γ_c' by equation (34) or (35)
	Updating acceleration orders as a_{yc}' and a_{zc}' by equation (36)
Else	
Step 4	Calculating γ^* from equation (21)
	Updating rolling angle order as γ_c' by equation (37)
	Updating the expected yawing angle as ϕ_c by equation (38)
	Generating new acceleration orders by equation (39)
End If	
Step 5	Guidance order rewritten in body frame as equation (40)

Step 5. Guidance order rewritten in missile body frame as

$$\begin{cases} a_{ybc} = a_{yc}' \cos\gamma + a_{zc}' \sin\gamma, \\ a_{zbc} = a_{zc}' \cos\gamma - a_{yc}' \sin\gamma. \end{cases} \tag{40}$$

Finally, a_{ybc}, a_{zbc}, and γ_c' are input of missile autopilot. The strategy ends.

Table 1 gives a complete algorithm of the guidance strategy maintaining minimum FOV angle constraint.

4. Numerical Simulations

In this section, the effectiveness of the proposed guidance strategy is demonstrated by numerical simulations, in which a hypersonic missile is considered to intercept a stationary target. The simulation adopts 3D kinematic model proposed. Considering the influence of attack angle and sideslip angle, the following aerodynamic model is introduced in simulation:

$$\begin{cases} F_x = C_D qS = \left(C_{D0} + C_D^{\alpha^2}\alpha^2\right) qS, \\ F_y = C_L qS = C_L^{\alpha}\alpha qS, \\ F_z = C_Z qS = C_Z^{\beta}\beta qS, \end{cases} \tag{41}$$

where F_x, F_y, F_z, q, and S represent drag, lift, lateral force, dynamic pressure, and reference area. α and β represent attack angle and sideslip angle. C_{D0}, $C_D^{\alpha^2}$, C_L^{α}, and C_Z^{β} are all aerodynamic force coefficient.

Typical values of basic parameters in the aerodynamic model are set in Table 2.

The basic guidance law adopted in simulation is demonstrated by equation (27). In order to simulate dynamic lag, first-order autopilot lag [9] is presented in all of three channels, shown as the following equation.

Table 2: Aerodynamic parameters used in simulation.

Parameters	Values	Parameters	Values
Mass (kg)	100	C_{D0}	0.08
$S\,(\mathrm{m}^2)$	0.1	$C_D^{\alpha^2}$	20.0
C_L^{α}	18.0	C_Z^{β}	-12.0

Table 3: Initial value setting of simulation.

Parameters	Values
Missile position (km)	(0, 30, 0)
Target position (km)	(50, 0, 10)
Missile velocity (m/s)	2000
Pitching angle	0°
Yawing angle	0°
Rolling angle	0°

$$\begin{cases} \dot{a}_{yb} = \dfrac{1}{\tau_\theta} a_{ybc} - \dfrac{1}{\tau_\theta} a_{yb}, \\ \dot{a}_{zb} = \dfrac{1}{\tau_\phi} a_{zbc} - \dfrac{1}{\tau_\phi} a_{zb}, \\ \dot{\gamma} = \dfrac{1}{\tau_\gamma} \gamma_c' - \dfrac{1}{\tau_\gamma} \gamma. \end{cases} \tag{42}$$

In equation (42), a_{ybc}, a_{zbc}, and γ_c' are inputs of pitching, yawing, and rolling autopilot. a_{yb} and a_{zb} are real acceleration in body frame which will be used in the kinematic model and be used to calculate real attack angle and sideslip angle.

Magnitudes of normal acceleration a_{yb} and a_{zb} are constrained within $\pm 100\mathrm{m/s}^2$ and $\pm 80\mathrm{m/s}^2$ to simulate physical limits of missile structure. Initial values of simulation scenario are listed as Table 3.

In order to simulate minimum FOV angle constraint caused by strapdown seeker, the range of seeker's FOV is limited. FOV in elevation direction ranges from −5° to −30° and in azimuth direction ranges from −15° to 15°.

Two simulation scenarios are compared as follows. Both of them adopt the above-mentioned simulation conditions. The first simulation does not use the proposed guidance strategy, in which the seeker loses the target in a long distance. In comparison, the second one adopts the proposed guidance strategy to sustain minimum FOV angle constraint.

4.1. Simulation Case without Guidance Strategy. In this simulation scenario, impact angle θ_f mentioned in guidance law (27) is determined as −50°. Simulation results are presented in Figure 7. From the 3D trajectory shown in Figure 7(a), we can see that the missile has heading error both in elevation and azimuth directions. Under the action of OGL on elevation guidance, terminal impact angle is controlled to −50° effectively. Without any specific guidance strategy, the missile flies in skid-to-turn (STT) mode and rolling angle order keeps 0. Lateral acceleration order is small in terminal guidance. In Figure 7(f), we can see how look angles change during the whole guidance flight. The azimuth angle σ_y converges to 0 very fast, compared with the elevation angle σ_z. But the absolute value of σ_z still decreases along with the missile approaching the target, which makes the minimum FOV constraint unmet finally. When the relative distance between missile and target is within 20 km, the absolute value of σ_z is less than the minimum FOV angle and after that the seeker loses the target.

4.2. Simulation Adopting Guidance Strategy. In order to prove the effectiveness of the mentioned guidance strategy, a simulation on the same condition of Section 4.1 is presented. The guidance strategy for maintaining minimum FOV angle constraint is used in this simulation. Threshold value of σ_z to trigger the strategy is 6° (absolute value) in consideration of dynamic lag. Simulation results are presented in Figure 8.

According to equation (10), the end point of seeker look angle control is calculated. Substituting the following values

$$\begin{cases} V = 2000\ (\mathrm{m/s}), \\ \sigma_{\min} = 6\ (^\circ), \\ a_{\max} = 100\ (\mathrm{m/s}^2) \end{cases} \tag{43}$$

into equation (10), it is obtained that

$$r_e = \frac{2000 \times 2000}{100} \times \sin 6^\circ \approx 4.2 \times 10^3 (\mathrm{m}). \tag{44}$$

The guidance strategy ends when the relative distance to target becomes 4.2 km. From Figure 8, we can see that the guidance strategy starts working when flight time is about 20 s (relative range 22 km). At this moment, σ_z reaches −6°, and it activates the strategy. Until it comes to the end point r_e, the guidance strategy controls σ_z lower than −6° very well, which is shown in Figure 8(f).

Figure 8(c) presents the missile's attitude angle change during flight. It is noticed that when the guidance strategy starts working heading error in azimuth direction has been eliminated. In order to compensate the look angle, the strategy forces the missile to maneuver in azimuth direction. Meanwhile, the missile starts rolling until look angle σ_z meets the miminum FOV angle constraint.

Acceleration orders are demonstrated in Figure 8(e). Two peaks appear when the guidance strategy starts and ends. The peak value of a_y at seeker look angle control end point is $-92(\mathrm{m/s}^2)$ which meets the normal acceleration constraint of $\pm 100(\mathrm{m/s}^2)$. This result proves the effectiveness of determining look angle control end point by equation (10).

Simulation results demonstrated by Figure 8 prove that this guidance strategy indeed maintains seeker look angle to meet the minimum FOV angle constraint during its working period. Compared with the simulation results shown in Figure 7, the strategy reduces the distance of seeker losing target from 22 km to 4.2 km, which is important to improve terminal guidance accuracy.

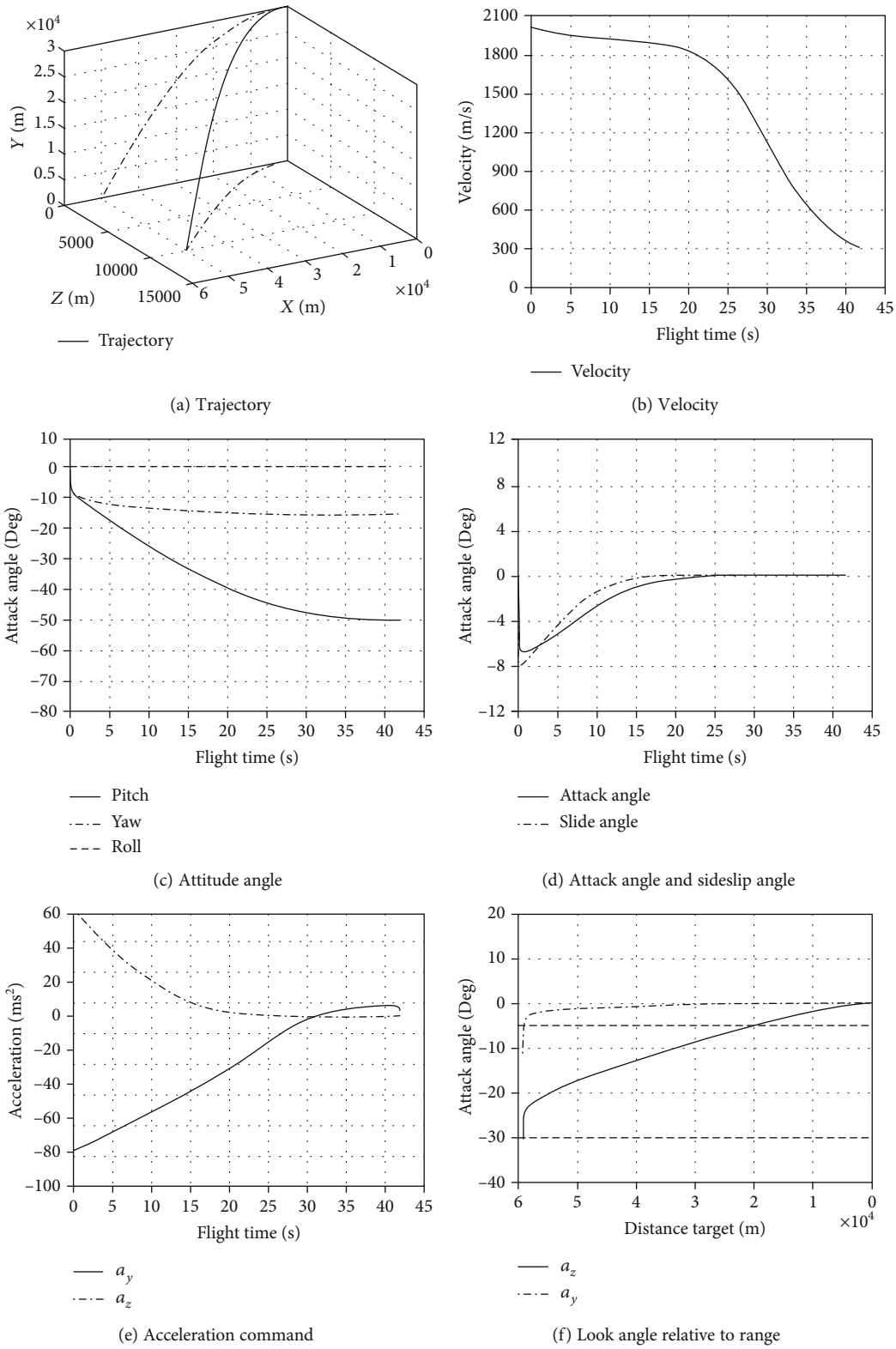

Figure 7: Simulation results without guidance strategy.

Moreover, simulation results show that impact angle is −50°. OGL works well in elevation guidance, and look angle compensation maneuver will not disturb impact angle control in terminal guidance. The guidance strategy proposed in this paper can be applied in scenario with impact angle constraint easily.

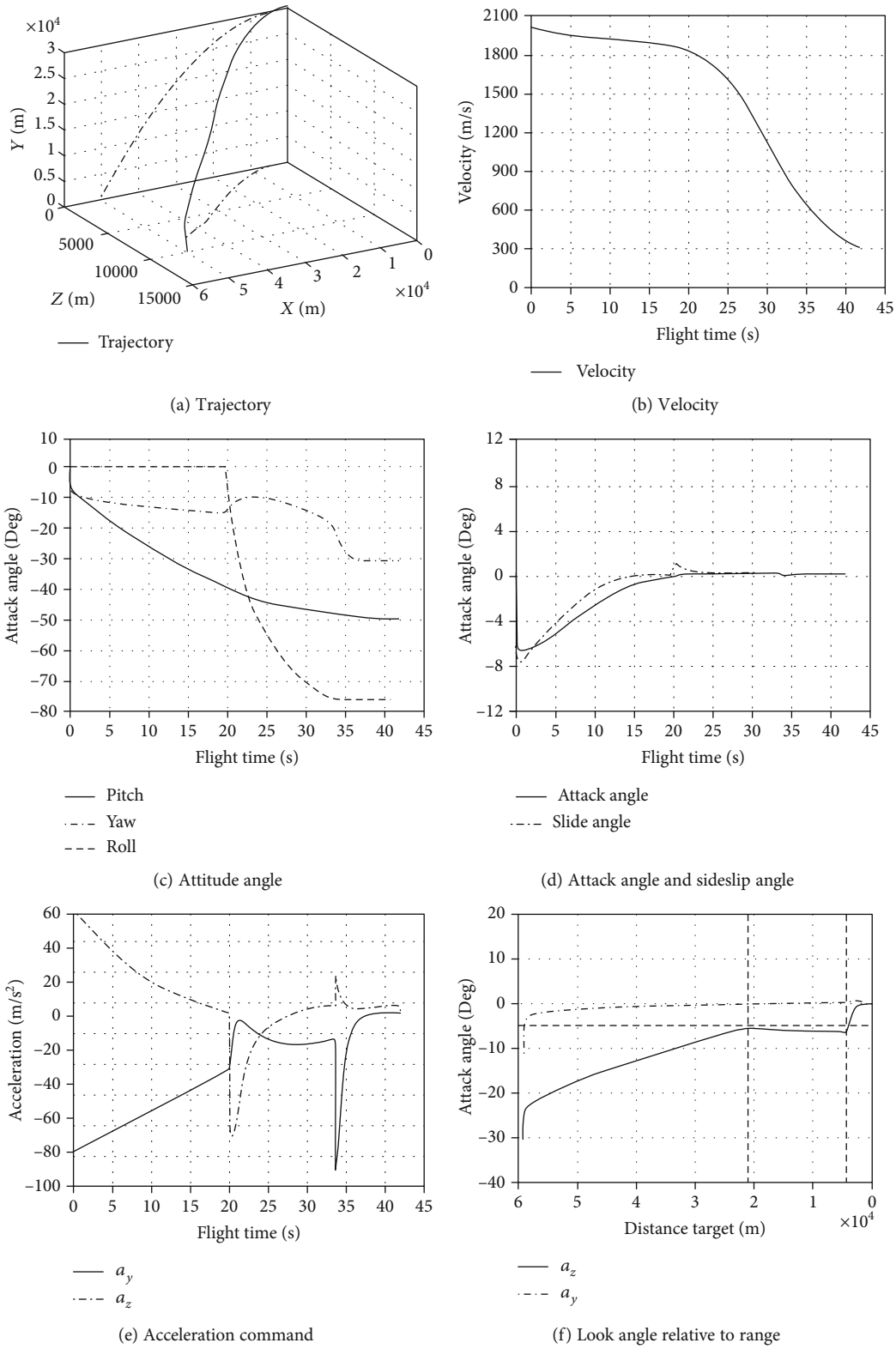

(a) Trajectory (b) Velocity

(c) Attitude angle (d) Attack angle and sideslip angle

(e) Acceleration command (f) Look angle relative to range

Figure 8: Simulation results adopting guidance strategy.

5. Conclusions

In this paper, a guidance strategy for strapdown seeker to sustain minimum FOV angle constraint is proposed. The problem of minimum FOV angle constraint is formulated at first. According to the analysis of engagement geometry, it is proven that this constraint will not be met within a finite acceleration at the end of trajectory when the missile attacks a

stationary target. The seeker look angle will come to 0 before or at the end time. The seeker loses the target finally. In order to reduce the distance of seeker losing target, a new guidance strategy is designed. It does not change the existing guidance law when the seeker look angle meets FOV constraint. Once the target is about to leave the seeker's FOV, the strategy takes effect. It sustains the minimum FOV angle constraint, by means of generating a new rolling order to keep the target in FOV and maneuvering in lateral to increasing heading error. Secondly, an end point of look angle control is defined and calculated, before which the guidance strategy will lay off and switch back to the original guidance law. This end point protects missile's acceleration from exceeding constraint. Lastly, simulations and comparisons are presented as verification. Simulation results show that the proposed guidance strategy maintains the seeker look angle within FOV during its working period without exceeding maximum acceleration restriction. The proposed guidance strategy is proven effective, and it reduces the distance of seeker losing target. This is to the benefit of increasing terminal guidance accuracy.

Data Availability

The data used in analysis and simulation are included within the article.

Conflicts of Interest

The authors declare that there is no conflict of interest regarding the publication of this paper.

References

[1] Q. Wen, Q. Xia, and W. Su, "A parameter design strategy for seeker's field-of-view constraint in impact angle guidance," *Proceedings of the Institution of Mechanical Engineers, Part G: Journal of Aerospace Engineering*, vol. 229, no. 13, pp. 2389–2396, 2015.

[2] R. Li, Q. Wen, W. Tan et al., "Adaptive weighting impact angle optimal guidance law considering seeker's FOV angle constraints," *Journal of Systems Engineering and Electronics*, vol. 29, no. 1, pp. 142–151, 2018.

[3] X. Chen and J. Wang, "Nonsingular sliding-mode control for field-of-view constrained impact time guidance," *Journal of Guidance, Control and Dynamics*, vol. 41, no. 5, pp. 1214–1222, 2018.

[4] H. G. Kim and H. J. Kim, "Backstepping-based impact time control guidance law for missiles with reduced seeker field-of-view," *IEEE Transactions on Aerospace and Electronic Systems*, vol. 55, no. 1, pp. 82–94, 2019.

[5] B. Liu, M. Hou, and D. Feng, "Nonlinear mapping based impact angle control guidance with seeker's field-of- view constraint," *Aerospace Science and Technology*, vol. 86, pp. 724–736, 2019.

[6] B. G. Park, T. H. Kim, and M. J. Tahk, "Optimal impact angle control guidance law considering the seeker's field-of-view limits," *Proceedings of the Institution of Mechanical Engineers, Part G: Journal of Aerospace Engineering*, vol. 227, no. 8, pp. 1347–1364, 2012.

[7] C. H. Lee, C. Hyun, and J. G. Lee, "A hybrid guidance law for a strapdown seeker to maintain lock-on conditions against high speed targets," *Journal of Electrical Engineering and Technology*, vol. 53, no. 3, pp. 1250–1260, 2017.

[8] D. K. Sang and M. J. Tahk, "Guidance law switching logic considering the seeker's field-of-view limits," *Proceedings of the Institution of Mechanical Engineers, Part G: Journal of Aerospace Engineering*, vol. 223, no. 8, pp. 1049–1058, 2009.

[9] Y. Ji, D. Lin, W. Wang, S. Hu, and P. Pei, "Three-dimensional terminal angle constrained robust guidance law with autopilot lag consideration," *Aerospace Science and Technology*, vol. 86, pp. 160–176, 2019.

[10] S. He and D. Lin, "Three-dimensional optimal impact time guidance for antiship missiles," *Journal of Guidance, Control and Dynamics*, vol. 42, no. 4, pp. 941–948, 2019.

[11] S. He, M. Kim, T. Song, and D. Lin, "Three-dimensional salvo attack guidance considering communication delay," *Aerospace Science and Technology*, vol. 73, pp. 1–9, 2018.

[12] C. K. Ryoo, H. Cho, and M. J. Tahk, "Optimal guidance laws with terminal impact angle constraint," *Journal of Guidance, Control and Dynamics*, vol. 28, no. 4, pp. 724–732, 2005.

[13] Z. Chen and T. Shima, "Nonlinear optimal guidance for intercepting a stationary target," *Journal of Guidance, Control and Dynamics*, vol. 42, no. 11, pp. 2418–2431, 2019.

[14] I. S. Jeon and J. I. Lee, "Optimality of proportional navigation based on nonlinear formulation," *IEEE Transactions on Aerospace and Electronic Systems*, vol. 46, no. 4, pp. 2051–2055, 2010.

[15] P. Zarchan, *Tactical and Strategic Missile Guidance*, AIAA, VA, 6th edition, 2012.

[16] T. Wang, S. Tang, J. Guo, and H. Zhang, "Two-phase optimal guidance law considering impact angle constraint with bearings-only measurements," *International Journal of Aerospace Engineering*, vol. 2017, Article ID 1380531, 12 pages, 2017.

[17] K. Becker, "Closed-form solution of pure proportional navigation," *IEEE Transactions on Aerospace and Electronic Systems*, vol. 26, no. 3, pp. 526–533, 1990.

[18] H. Q. Zhang, S. J. Tang, J. Guo, and W. Zhang, "A two-phased guidance law for impact angle control with seeker's field-of-view limit," *International Journal of Aerospace Engineering*, vol. 2018, Article ID 7403639, 13 pages, 2018.